The final version of this manuscript appeared in IEEE Transactions on Communications, vol.57, no.8, pp.2463-2473, Aug. 2009
DOI: 10.1109/TCOMM.2009.08.070662

A Mathematical Framework for the Performance Analysis of Bluetooth with Enhanced Data Rate

Andrea Zanella, *Member, IEEE,*

***Abstract*—In this paper, we present a mathematical framework that permits a detailed performance analysis of Bluetooth connections in fading channels. Conversely to most part of the literature, we distinguish between the transmission of useful and duplicate frames, which are handled in a different manner by the receiving unit. To this end, we define a two–state Markov Chain and we apply the renewal reward theory to determine the expressions of the throughput, energy efficiency and delay performance of the link. Although the model can be applied to any version of Bluetooth specifications, as a proof of concept we provide an accurate performance analysis of an asymmetric Bluetooth v2.0+EDR (Enhanced Data Rate) connection in typical propagation environments. The analysis reveals that best performance are (almost) always obtained by using the longest baseband frames transmitted at 2 Mbps in the low–to–medium signal–to–noise ratio (SNR) region, and at 3 Mbps in the high SNR region. Furthermore, we observed that it is more fruitful assigning the master role to the destination unit. The model, hence, proves to be a valuable tool to gain insights on the aspects that have a major impact on the system performance.**

***Index Terms*—Bluetooth, EDR, model, energy, throughput, delay, performance**

I. Introduction

One of the most attractive features of Bluetooth technology is the very low power consumption that permits its integration in portable, battery driven electronic devices, such as mobile phone, mouse, PDA and so on. As a matter of fact, Bluetooth standard defines four operational modes, namely *Active*, *Hold*, *Sniff*, and *Parked*. These modes correspond to different degrees of activity and, in turn, different levels of power consumption. Besides these high–level mechanisms, energy–saving is also pursued at a microscopic level, by means of a suitable packet reception mechanism that permits a device to switch off the receiver circuitry as soon as it realizes that the incoming signal cannot be correctly decoded or it is addressed to another device. In this way, a unit that is not addressed by any valid packet is active for less than 10% of the time.

Despite this very attractive low–power feature, some implementation and compatibility problems have slowed down the penetration of the Bluetooth technology in the market, until recently. Most of such problems are now solved and Bluetooth is undertaking the expected success, being integrated in hundreds of portable electronic devices. However, the first generation of Bluetooth products, compliant with the Bluetooth v1.1 specifications [1], was characterized by a low transmission rate (1 Mbps) and a rather long connection set–up time (order of seconds), which have restricted the use of Bluetooth mainly to cable–replacement applications. These limitations have been partially removed by the enhancements included in the Bluetooth v2.0+EDR specifications [2]. The new version of the standard, in fact, includes an Enhanced Data Rate (EDR) mode for higher transmission rates (up to 3 Mbps) together with other improvements aimed at speeding up the node discovery and connection setup procedures and limiting the interference with other devices operating in the same frequency band. In February 2007, moreover, the Bluetooth Special interest Group published the last update of the standard, Bluetooth v2.1 + EDR [3], which contains further improvements to the link establishment procedure. With these upgrades, Bluetooth is ready to break through the borders of cable–replacement products and enter the wide arena of high–speed radio technologies and pervasive networks. This enlarged and challenging scenario includes different types of applications, such as opportunistic data exchange, bulk data transfer, distributed and cooperative computing and storage and so on [4].

The success of Bluetooth in these competitive areas, however, depends on the actual performance, in terms of throughput, delay and energy efficiency, that the technology can provide in realistic propagation environments. This topic has been partially addressed by previous work. In [5], the authors investigate some techniques to improve Bluetooth EDR data throughput by using forward error correction and interleaving schemes. However, the study does not present any delay and energy efficiency analysis. The point–to–point Bluetooth throughput achieved by 1 Mbps frame formats is derived in [6]–[8] for different channel conditions. A mathematical approach to the performance analysis of Bluetooth piconet can be found, for instance, in [9]–[16]. The aim of such works, however, is to model the general performance trend of the system, in order to permit a comparative analysis of different polling and retransmission strategies, rather than providing accurate results for throughput and energy efficiency. Segmentation–&–Reassembly (SAR) policies are investigated in [17], [18], where throughput is still considered as the only performance metric. Some discussions on the energy efficiency aspects of the Bluetooth system can be found in [19] and references therein. Such works are mainly focused on the definition of dynamic power management policies, which reduce the energy consumption by using the low power modes provided by the standard. However, the energy consumption during active data exchange and for different channel conditions is not investigated.

All the cited papers, as well as most of the other works concerning Bluetooth performance analysis, are based on a simplified model of the Bluetooth reception procedure that

A. Zanella is with the Department of Information Engineering, University of Padova, Padova, 35131 Italy e-mail: zanella@dei.unipd.it

neglects some details defined by the standard. Although these simplifications might be acceptable for comparing different high–level protocols, they become critical when looking at the link–layer performance, in general, and at the energy efficiency, in the specific. Therefore, in this paper we propose a novel mathematical model that takes into consideration the microscopic–level energy saving mechanisms defined by the Bluetooth specifications and permits an accurate analysis of the throughput, delay and energy efficiency achieved by the different baseband frame formats at the link layer.

More specifically, we analyze the events that occur during active frame exchange and we determine the average energy consumed by each unit, the amount of transferred data and the time taken by the process. Then, applying the renewal reward theorem and the first–step analysis, we derive the throughput, delay and energy efficiency performance metrics.

As a case study, we apply the mathematical model to a Bluetooth v2.0+EDR asynchronous data link and we derive the system performance for different values of the signal to noise ratio in Rayleigh fading radio channels.

The contribution provided by this work, hence, is twofold. First, we provide a complete performance model for Bluetooth data link in active mode. Second, we present a case study in which we apply the mathematical framework to a Bluetooth v2.0+EDR link and we derive the throughput, delay and energy efficiency figures of different frame formats in typical radio propagation environments. A preliminary version of this work appeared in [20]. That work is here enriched by the definition and analysis of new performance indexes, such as packet delivery delay statistics and energy balancing, and by a thorough investigation of the impact of the master/slave role assignment in asymmetric connections.

The remainder of this paper is organized as follows. Sec. II provides an overview of the Bluetooth radio system. In Sec. III, we describe the mathematical model for an ACL data link and we derive the reward functions that are used in Sec. IV to define the performance metrics. Sec. V presents the results obtained for the case study. Finally, Sec. VI concludes the paper with some final remarks.

II. Bluetooth v2.0 + Enhanced Data Rate

This section shortly overviews the features of the Bluetooth v2.0+EDR standard that are of interest for our analysis. An introductory description of the main features of Bluetooth technology can be found in [21], whereas for the details we refer the reader to the official standard [3].

A. Physical layer: basic and enhanced data rate modes

The Bluetooth v2.0+EDR specifications encompass three modulation schemes, which correspond to a basic data rate of $R_1 = 1$ Mbps (BR), and two enhanced data rate modes of $R_2 = 2$ Mbps (2EDR) and $R_3 = 3$ Mbps (3EDR), respectively. The BR mode makes use of a binary Gaussian–shape Frequency Shift Keying scheme (GFSK), while 2EDR and 3EDR are obtained by using Differential encoded Phase Shift Keying (DPSK) modulations, with a constellation of four symbols ($\pi/4$–DQPSK) and eight symbols (8DPSK), respectively. In all the cases, the symbol period remains equal to $T_s = 1\,\mu\,s$, so that the frequency band of the radio signal is not significantly modified by the introduction of the EDR schemes.

The expressions of the bit error rate (BER) for the three modulation schemes can be found, for instance, in [22]–[24]. For reader convenience, we have collected them in [25], together with the expressions of the frame reception events that will be described later. For a given Signal–to–Noise Ratio (SNR), defined as the ratio between the average energy per symbol E_s and the noise energy N_0, the BER of GFSK and $\pi/4$–DQPSK modulations is very similar, so that the last scheme is always preferable, giving a transmission rate that is twice the basic one. This performance gain is payed in terms of transceiver complexity. For instance, the basic–rate GFSK scheme, being a constant–envelope modulation, permits to have the amplifier working in proximity of the saturation point, where it is most efficient. Conversely, DPSK modulation schemes have a peak to average ratio of about 3.3 dB, which requires to move the working point of the amplifier below the saturation point, in order to avoid clipping effects. Therefore, to maintain the same output power, more efficient amplifiers have to be used.

In the light of this consideration, the rest of this paper will be focused on EDR schemes only. Reader interested on the performance analysis for the basic rate packet formats are referred to [8], [11], [26].

B. ACL baseband frame formats

The Bluetooth standard encompasses two types of links: Synchronous Connection Oriented (SCO) and Asynchronous ConnectionLess (ACL). SCO links are aimed at the transport of delay–sensitive traffic (mainly voice) and make use of a periodical time–reservation scheme. ACL links are intended for the transport of asynchronous data traffic, as generated by file transfer and web browsing applications. In the following of this paper we focus on ACL links only.

Table I
Characteristics of ACL data frames

Type	Slots	Rate [Mbps]	PAYLOAD [bytes] header	data	CRC	FEC rate
POLL	1	1	1	–	–	–
NULL	1	1	1	–	–	–
$2DH1$	1	2	2	54	2	–
$2DH3$	3	2	2	367	2	–
$2DH5$	5	2	2	679	2	–
$3DH1$	1	3	2	83	2	–
$3DH3$	3	3	2	552	2	–
$3DH5$	5	3	2	1021	2	–

Bluetooth v2.0+EDR adds six ACL frame formats to the basic rate formats introduced in the first version of the standard. Each ACL data frame begins with an Access Code (AC) field that is used for synchronization, DC offset compensation and piconet identification. AC is followed by the frame header (HEAD) field, which contains link control information, including frame type, destination address, sequence number, and acknowledgment flag. Furthermore, the HEAD field contains a checksum word (HEC) which is used to verify the integrity of the field after decoding. For backward compatibility, AC and HEAD fields are always transmitted at the basic rate.

In EDR frames, the HEAD is followed by a guard time of approx $5\,\mu s$, which is used to switch the transceiver circuitry to the appropriate DPSK scheme. The guard time is followed by a synchronization field (SYNC) of 10 DPSK–modulated symbols that is used for signal acquisition at the receiver. The SYNC is followed by a variable–length PAYL field, which includes a 2–byte header and a 2–byte CRC subfield. The last field of the frame is the EDR Trailer of only 2 symbols. SYNC, PAYL and Trailer fields are transmitted by using the selected EDR modulation scheme. The time occupancy of EDR frames is limited to 1, 3 or 5 consecutive slots. The different EDR frame formats are denoted by $jDHn$, where $j = 2, 3$ is the transmission rate (in Mbps), while $n = 1, 3, 5$ is the slot occupancy.

Besides these data frames, Bluetooth specifications define two short control frames, named POLL and NULL, which contain AC and HEAD fields only with no PAYL.

The characteristics of the different frame formats are summarized in Tab. I.

C. Baseband

The basic Bluetooth network configuration is the so–called piconet, a cluster of no more than eight devices sharing a common frequency–hopping radio channel. When the piconet is established, one unit gets the *master* role, while the others get the *slave* role. The master is in charge to manage the medium access by means of a polling scheme: the master cyclically polls the slave by sending either useful data frames or POLL frames. The slave addressed by the master frame is required to immediately return a data or NULL frame.

Bluetooth provides a reliable data connection by using a Stop&Wait Automatic Retransmission Query (ARQ) mechanism at the baseband layer. Each data frame is transmitted and retransmitted until the source node gets a positive acknowledgment (ACK) from the destination. The ACK is carried in the HEAD field of the baseband frame (piggy–backing), so that its reception probability is independent of the frame format. Since negative ACK is assumed by default, master retransmissions are also triggered by ACK losses. In particular, the loss of frames carrying positive ACKs will trigger the retransmission of frames that had already been successfully delivered to the slave. These frames are called *duplicate packets* (DUPCKs). When a slave receives a frame, it checks whether the sequence number in the HEAD field has been changed since the last useful frame received from the master. If not, the slave recognizes the incoming frame as a DUPCK and returns a positive ACK, irrespective of the actual reception state of the payload field. Notice, that slave transmissions are allowed only upon receiving a valid master's frame that, in turn, will also carry the (positive or negative) acknowledgment for the previous slave–to–master transmission. Therefore, slaves retransmissions occur only when solicited by an explicit not acknowledgment sent by the master.

D. Micro–level energy saving mechanisms

Energy–saving was a key feature in the design of the Bluetooth technology. According to this principle, a unit stops receiving and enters a low–power *doze mode* as soon as it determines that a field in the incoming frame is affected by unrecoverable errors or the frame is addressed to another unit (see [1], Volume 1, pg. 124, and [3], Vol. 2, pg. 174).

More specifically, at the beginning of each receive slot, the Bluetooth unit scans the received radio signal looking for a valid AC field. If the AC is not recognized within a proper time window, reception stops and the unit enters a low–power *doze mode* until the beginning of the following receive slot. Conversely, after the recognition of the AC field, the receiver processes the HEAD field and checks the validity of the HEC word. If the check fails, the device enters doze–mode, otherwise the HEAD field is inspected to determine the frame format and the destination address. Slaves not addressed by the master transmission may enter doze–mode till the end of the frame. The slave addressed by the master, instead, checks the sequence number contained in the HEAD field of the incoming frame to verify whether it is a DUPCK or not. In the first case, the remaining of the frame is not decoded and the slave enters doze mode till the end of the transmission, after which it piggy–backs a positive acknowledgment to the master. When the incoming frame is not a DUPCK, instead, the slave decodes the entire frame and, then, it piggy backs a positive or negative ACK according to the outcome of the CRC of the PAYL field.

III. ACL Data Link Model

In this section, we define the mathematical model that permits an accurate performance analysis of a Bluetooth ACL connection. To this end, we need first to introduce some notations and hypotheses. Then, we define a Markov model used to describe the system evolution and we briefly outline the basis of the renewal reward theory. Finally, we determine the average reward functions that will be successively used to determine the performance indexes of interest.

For the sake of simplicity, we limit the study to the case of a piconet with only two units: one master and one slave. The extension of the analysis to the multi–slave case, which requires a more cumbersome notation and exposition, is briefly discussed in Appendix.

A. Notation

As explained in Sec. II-D, the reception of a baseband frame is performed in three consecutive steps corresponding to: 1) Access code acquisition (A); 2) frame Header recognition (H); 3) Data (payload) reception (D). If one of such step fails, then the unit enters power saving mode, skipping the remaining reception steps.

The success or failure of a given reception step will be denoted by adding the subscript s and f, respectively, to the step symbol. For instance, H_f denotes the case in which AC acquisition step is correctly concluded but HEAD decoding fails. Notice, that the different reception events meet the following relations:

$$A_s = \neg A_f\,; \quad A_s = H_s \cup H_f\,; \quad H_s = D_s \cup D_f\,; \qquad (1)$$

where the symbols $\neg$ and $\cup$ denote the complementary and union operators, respectively. Furthermore, we will denote by P_X the probability of the generic reception event X. Hence, according to (1), the following relations must hold

$$\begin{aligned} \mathrm{P}_{A_s} &= 1 - \mathrm{P}_{A_f} \\ \mathrm{P}_{A_s} &= \mathrm{P}_{H_s} + \mathrm{P}_{H_f} \\ \mathrm{P}_{H_s} &= \mathrm{P}_{D_s} + \mathrm{P}_{D_f} \end{aligned} \qquad (2)$$

When necessary, we add the superscript (M) and (S) to distinguish between master and slave unit, respectively. For example, $\mathrm{P}^{(\mathrm{M})}_{D_f}$ denotes the probability of receiving a master's frame with valid AC and HEAD fields and unrecoverable errors in the PAYL field. Notice, that the reception probabilities for the AC and HEAD fields, which are always transmitted at the basic rate, do not depend on the frame format. Conversely, P_{D_s} and P_{D_f} depend on the frame format, though this dependency does not appear in the notation, to reduce clutter.

The probability functions depend on the characteristics of the Bluetooth receiver and on the channel model considered. For space constraints, we do not report here their expressions that can be found, for instance, in [8]. Furthermore, for reader convenience, we have collected all the equations used in this paper into a public available technical report [27].

B. Assumptions

We consider a heavy traffic scenario, where master and slave have always packets waiting for transmission. We assume infinite retransmission timeout: packets are retransmitted over and over again until the sender receives a positive acknowledgment. In order to determine the performance achieved by the different baseband frame formats, we consider a static Segmentation and Reassembly (SAR) policy that makes use of a single frame format per connection. Concerning the radio channel, we assume the classical WSSUS (Wide–Sense Stationary Uncorrelated Scattering) slow flat Rician fading model [28], so that, by virtue of the frequency hopping mechanism, frames are subject to statistically independent flat fading.

Notice, that a node can determine the end of an ongoing transmission by inspecting the information contained in the HEAD field of the frame. However, we assume that, if the packet is not recognized because of unrecoverable errors in the AC or HEAD fields, the node is still capable of determining the end of the ongoing transmission by measuring the Received Signal Strength (RSS) at the antenna. Although this carrier sensing mechanism is not explicitly required by the Bluetooth specifications, it is now provided by the last generation Bluetooth chipsets [29]. In any case, the mathematical framework we provide may be very easily adapted to the case in which carrier–sensing is not supported, as done in [25].

C. Markovian Model

Under the considered hypotheses, the dynamic of the system can be captured by means of a Markov Chain (MC) with two states: *Normal* (N) and *Duplicate* (D). In state N, the master transmits new downlink frames or retransmit frames that have never been correctly received by the slave. The system leaves the N state to enter state D whenever the master does not recognize a slave's frame carrying a positive acknowledgment. Therefore, the transition probability P_{ND} from state N to D is given by

$$P_{\mathrm{ND}} \quad = \quad \mathrm{P}^{(\mathrm{M})}_{D_s}(1 - \mathrm{P}^{(\mathrm{S})}_{H_s}) \qquad (3)$$

In state D, the master keeps transmitting duplicate packets. State D is left when the master finally gets a positive acknowledgment from the slave. Since the slave disregards the PAYL field of DUPCKs, the transition probability P_{DN} from state D to N is given by

$$P_{\mathrm{DN}} \quad = \quad \mathrm{P}^{(\mathrm{M})}_{H_s}\mathrm{P}^{(\mathrm{S})}_{H_s} \qquad (4)$$

The steady state probabilities π_{N} and π_{D} of the MC being in states N and D, respectively, are then given by

$$\pi_{\mathrm{N}} = \frac{P_{\mathrm{DN}}}{P_{\mathrm{ND}} + P_{\mathrm{DN}}}\,; \quad \pi_{\mathrm{D}} = \frac{P_{\mathrm{ND}}}{P_{\mathrm{ND}} + P_{\mathrm{DN}}} \qquad (5)$$

D. Reward functions

Following the approach suggested in [30], Bluetooth performance can be investigated by resorting to the classical theory of renewal reward processes [31]. Consider two generic reward functions, $R^{(1)}$ and $R^{(2)}$, such that $R^{(1)}_j$ and $R^{(2)}_j$ are the average reward earned each time the Markov chain enters in state $j \in \mathbf{E}$. Furthermore, let $R^{(1)}(\tau)$ and $R^{(2)}(\tau)$ be the total reward earned through the system evolution in the interval $[0, \tau]$, so that, denoting by $I_j(\tau)$ the number of times state j is entered in the time interval $[0, \tau]$, we have

$$R^{(h)}(\tau) = \sum_{j \in \mathbf{E}} R^{(h)}_j I_j(\tau)\,; \quad h = 1, 2$$

A fundamental result of renewal theory [32] states that the ratio between the two reward functions asymptotically equals the ratio of the statistical reward averages $\bar{R}^{(1)}$ and $\bar{R}^{(2)}$. In formula, we have

$$\lim_{\tau\to\infty} \frac{R^{(1)}(\tau)}{R^{(2)}(\tau)} = \lim_{\tau\to\infty} \frac{\sum_{j\in\mathbf{E}} R^{(1)}_j I_j(\tau)}{\sum_{j\in\mathbf{E}} R^{(2)}_j I_j(\tau)} = \frac{\sum_{j\in\mathbf{E}} \pi_j R^{(1)}_j}{\sum_{j\in\mathbf{E}} \pi_j R^{(2)}_j} = \frac{\bar{R}^{(1)}}{\bar{R}^{(2)}} \qquad (6)$$

where π_j is the steady state probability of the chain being in state j. Thanks to this result, we can derive a number of performance indexes from the statistical average of a selection of suitable reward functions. In particular, we consider the following functions:

- state transition time, $\overline{T}$;
- average number of successfully delivered data bits, $\overline{D}$;
- amount of consumed energy, $\overline{W}$.

In order to derive the expected values of these reward functions, we need to introduce some further notations. Let

$w_{TX}(X)$, $w_{RX}(X)$ and $w_{SS}(X)$ be the amount of energy consumed by a unit for transmitting, receiving and *sensing*, respectively, the generic packet field X. Let $jDHn$ and $iDHm$, with $n, m \in \{1, 3, 5\}$ and $i, j \in \{2, 3\}$, be the packet types used by the master and slave units, respectively. Finally, let $\mathbb{D}(h, k)$ be the number of useful data bits carried by the generic $hDHk$ frame, as reported in the `data` column of Tab. I.

Time Reward

The transmission of a $jDHn$ frame by the master always takes n time slots. In order to reply with an $iDHm$ frame, the slave needs to decode at least the AC and HEAD fields of the master frame. In this case, the uplink phase will take m slots. Otherwise, the slave is not allowed to transmit and the uplink phase takes only one slot. The average *time* reward earned per MC transition is, then, equal to

$$\overline{T} = n + 1 + \mathrm{P}_{H_s}^{(\mathrm{M})}(m - 1) \tag{7}$$

Data Reward

In state N, the master transmits useful frames, i.e., frames that have not been correctly received by the slave yet. Therefore, in state N, the successful reception of a master's frame by the slave brings about a data reward of $\mathbb{D}(j, n)$. Notice, that the reward is earned even whether the positive ACK returned by the slave is not received by the master. In this case, however, the master will enter the duplicate state D and start transmitting DUPCKs, which do not carry useful information and, hence, do not yield any reward. The slave unit, in turn, gains a data reward of $\mathbb{D}(i, m)$ whenever it correctly decodes the header of a master frame (thus being allowed to transmit its own frame) and its frame is successfully decoded by the master. Summing up, the average number of data bits successfully delivered by the master and slave units, respectively, in a MC step is given by

$$\overline{D}^{(\mathrm{M})} = \pi_{\mathrm{N}} \mathrm{P}_{D_s}^{(\mathrm{M})} \mathbb{D}(j, n) \tag{8}$$

$$\overline{D}^{(\mathrm{S})} = \mathrm{P}_{H_s}^{(\mathrm{M})} \mathrm{P}_{D_s}^{(\mathrm{S})} \mathbb{D}(i, m) \tag{9}$$

Energy Reward

The computation of the energy spent by the master and slave units for each transition step of the MC, though cumbersome, is not complicated.

At each step of the MC, the master spends $w_{TX}(jDHn)$ energy units to transmit its frame and some energy to decode the slave's reply (if any). More specifically, if the slave does not recognize the master polling (probability $1 - \mathrm{P}_{H_s}^{(\mathrm{M})}$), then no frame is returned, so that the master reception phase is concluded after that the channel has been sensed idle for a time period equal to the AC duration. Conversely, when an $iDHm$ frame is returned, the master starts decoding the incoming bitstream, unless unrecoverable errors occur during the reception of the AC or HEAD fields. In this case, the master stops decoding and keeps sensing the channel till the end of the slave's transmission. Therefore, the average amount of energy spent by the master is given by

$$\begin{aligned}\overline{W}^{(\mathrm{M})} &= w_{TX}(jDHn) + \mathrm{P}_{H_s}^{(\mathrm{M})} \mathrm{P}_{H_s}^{(\mathrm{S})} w_{RX}(iDHm) \\ &+ \mathrm{P}_{H_s}^{(\mathrm{M})} \mathrm{P}_{H_f}^{(\mathrm{S})} \left[w_{RX}(AC + HEAD) + w_{SS}(PAYL^{(\mathrm{S})}) \right] \\ &+ \mathrm{P}_{H_s}^{(\mathrm{M})} \mathrm{P}_{A_f}^{(\mathrm{S})} \left[w_{RX}(AC) + w_{SS}(HEAD + PAYL^{(\mathrm{S})}) \right] \\ &+ (1 - \mathrm{P}_{H_s}^{(\mathrm{M})}) w_{SS}(AC)\end{aligned} \tag{10}$$

The energy spent by the slave unit can be obtained in a similar way, taking into consideration that slaves are not required to receive the PAYL field of DUPCKs and, as usual, the slave needs to sense the channel in order to recognize the end of the transmission in case of AC or HEAD errors. Therefore, after some algebra, we get

$$\begin{aligned}\overline{W}^{(\mathrm{S})} = &w_{RX}(AC) + \mathrm{P}_{A_s}^{(\mathrm{M})} w_{RX}(HEAD) + \\ &+ \mathrm{P}_{H_s}^{(\mathrm{M})} \pi_{\mathrm{N}} w_{RX}(PAYL^{(\mathrm{M})}) + (1 - \mathrm{P}_{H_s}^{(\mathrm{M})}) w_{SS}(PAYL^{(\mathrm{M})}) \\ &+ \mathrm{P}_{A_f}^{(\mathrm{M})} w_{SS}(HEAD) + \mathrm{P}_{H_s}^{(\mathrm{M})} w_{TX}(iDHm)\end{aligned} \tag{11}$$

IV. Performance metrics

Replacing the generic average reward functions $\bar{R}^{(1)}$ and $\bar{R}^{(2)}$ (6) with the time, energy or data rewards derived in the previous section we get a number of different performance indexes, among which we selected the following ones.

A. Goodput

The goodput $\mathcal{G}$ provides a measure of the average transmission capacity that the baseband layer offers to the higher protocols. The system goodput is defined as the average amount of successfully delivered data bits per unit of time and it is given by

$$\mathcal{G} = \frac{\overline{D}^{(\mathrm{M})} + \overline{D}^{(\mathrm{S})}}{\overline{T}} \tag{12}$$

B. Energy Efficiency

The energy efficiency ξ is defined as the average amount of successfully delivered data bit (in any direction) per unit of energy [33]. Thus, the overall system efficiency can be expressed as

$$\xi = \frac{\overline{D}^{(\mathrm{M})} + \overline{D}^{(\mathrm{S})}}{\overline{W}^{(\mathrm{M})} + \overline{W}^{(\mathrm{S})}} \tag{13}$$

C. Energy Balance

The system lifetime is defined as the average time the system can operate in active state before a unit depletes its battery. Normally, the energy consumption differs from master and slave. Therefore, energy efficiency ξ being equal, the system lifetime is extended when the energy consumption of master and slave units is balanced. To quantify this aspect, we introduce the energy–balancing index, defined as follows

$$\zeta = \left| \frac{\overline{W}^{(\mathrm{M})} - \overline{W}^{(\mathrm{S})}}{\overline{W}^{(\mathrm{S})} + \overline{W}^{(\mathrm{M})}} \right|$$

The closer ζ to 0, the more balanced the energy consumption between master and slave and, consequently, the longer the system lifetime.

D. Packet delay statistics

The last performance index considered in this work is related to the delivery delay τ of a protocol data unit (PDU) generated by the Logical Link Control and Adaptation Protocol (L2CAP), which lies directly upon the baseband layer. In particular, we are interest in the mean m_τ and variance ${\sigma_\tau}^2$ of such a time. In general, each L2CAP PDU will be fragmented into a number n of (possibly different) baseband frames, according to the Segmentation–&–Reassembly (SAR) policy. The PDU delay τ is, then, given by the sum of the service time y_i required to successfully delivering each of the baseband frames:

$$\tau = \sum_{i=1}^{n} y_i$$

Due to the statistical independence of these random variables, the first and second order moments of τ are given by:

$$m_\tau = \sum_{i=1}^{n} m_{y\,i} \tag{14}$$

$${\sigma_\tau}^2 = \sum_{i=1}^{n} \sigma^2_{y\,i} \tag{15}$$

where m_y and σ_y^2 are mean and variance, respectively, of the baseband service delay y.

The mean baseband service times $m_y^{(\mathrm{M})}$ and $m_y^{(\mathrm{S})}$ seen by the master and slave unit, respectively, can be obtained as follows:

$$m_y^{(\mathrm{M})} = \frac{\mathbb{D}(j,n)}{\overline{D}^{(\mathrm{M})}}\overline{T} = \frac{\overline{T}}{\pi_{\mathrm{N}} \mathrm{P}^{(\mathrm{M})}_{D_s}} \tag{16}$$

$$m_y^{(\mathrm{S})} = \frac{\mathbb{D}(i,m)}{\overline{D}^{(\mathrm{S})}}\overline{T} = \frac{\overline{T}}{\mathrm{P}^{(\mathrm{M})}_{H_s}\mathrm{P}^{(\mathrm{S})}_{D_s}} \tag{17}$$

where $\overline{D}^{(\mathrm{M})}$ and $\overline{D}^{(\mathrm{S})}$ are given by (8) and (9), respectively.

To determine the variance of y, instead, we need to resort to a first–step analysis.

Let us first focus on the baseband service time seen by the master. We notice that, whenever a new baseband frame is loaded into the transmission buffer, the MC is in state N. The transmission takes a time equal to $n + m$ if the frame header is recognized by the slave ($H_s^{(\mathrm{M})}$ event) and $n + 1$ otherwise. If the frame is not successfully acknowledged, then it will be retransmitted. The retransmission can occur with the MC in state N or D, depending on the outcome of the first transmission attempt. Let y_N and y_D denote the corresponding residual service time, i.e., the time to complete the service given that the first attempt has failed and the MC state is N or D, respectively. Furthermore, let χ_A be the indicator function for the event A, so that $\chi_A = 1$ when A holds true and $\chi_A = 0$ otherwise. Then, the baseband service time can be expressed as follows

$$\begin{aligned} y^{(\mathrm{M})} &= n+1+(m-1)\chi_{H_s^{(\mathrm{M})}} + (1-\chi_{D_s^{(\mathrm{M})}})y_N^{(\mathrm{M})} \\ &\quad + \chi_{D_s^{(\mathrm{M})}}(1-\chi_{H_s^{(\mathrm{S})}})y_D^{(\mathrm{M})} \end{aligned} \tag{18}$$

Due to the memoryless property of the MC, the random variables $y^{(\mathrm{M})}$ and $y_N^{(\mathrm{M})}$ have the same distribution. Therefore, by rising to the square both sides of (18) and taking the expectation of all the terms, after some algebra we get

$$\begin{aligned} M_y^{(\mathrm{M})} = & \frac{(n+1)^2 + (m-1)\mathrm{P}^{(\mathrm{M})}_{H_s} + 2(n+1)(m-1)\mathrm{P}^{(\mathrm{M})}_{H_s}}{\mathrm{P}^{(\mathrm{M})}_{D_s}} \\ & + \frac{(1-\mathrm{P}^{(\mathrm{S})}_{H_s})\mathrm{P}^{(\mathrm{M})}_{D_s}\left[M^{(\mathrm{M})}_{y_D} + 2m^{(\mathrm{M})}_{y_D}(n+m)\right]}{\mathrm{P}^{(\mathrm{M})}_{D_s}} \\ & + \frac{2m_y^{(\mathrm{M})}\left[(n+m)\mathrm{P}^{(\mathrm{M})}_{D_f} + (n+1)(1-\mathrm{P}^{(\mathrm{S})}_{H_s})\right]}{\mathrm{P}^{(\mathrm{M})}_{D_s}} \end{aligned} \tag{19}$$

where $M_y^{(\mathrm{M})}$ is the statistical power of $y^{(\mathrm{M})}$ and $y_N^{(\mathrm{M})}$, while $m^{(\mathrm{M})}_{y_D}$ and $M^{(\mathrm{M})}_{y_D}$ are the statistical mean and power of $y_D^{(\mathrm{M})}$, respectively. These last statistics, in turn, can be obtained by applying the first–step analysis to the transmission process from state D. In fact, on the basis of the above rational, the residual service time $y_D^{(\mathrm{M})}$ can be expressed as

$$y_D^{(\mathrm{M})} = n+1+(m-1)\chi_{H_s^{(\mathrm{M})}} + (1-\chi_{H_s^{(\mathrm{M})}}\chi_{H_s^{(\mathrm{S})}})\tilde{y}_D^{(\mathrm{M})} \tag{20}$$

where $y_D^{(\mathrm{M})}$ and $\tilde{y}_D^{(\mathrm{M})}$ are identically distributed. Hence, we easily get

$$m^{(\mathrm{M})}_{y_D} = \frac{n+1+(m-1)\mathrm{P}^{(\mathrm{M})}_{H_s}}{\mathrm{P}^{(\mathrm{M})}_{H_s}\mathrm{P}^{(\mathrm{S})}_{H_s}} \tag{21}$$

$$\begin{aligned} M^{(\mathrm{M})}_{y_D} = & \frac{(n+1)^2 + (m-1)\mathrm{P}^{(\mathrm{M})}_{H_s} + 2(n+1)(m-1)\mathrm{P}^{(\mathrm{M})}_{H_s}}{\mathrm{P}^{(\mathrm{M})}_{H_s}\mathrm{P}^{(\mathrm{S})}_{H_s}} \\ & + \frac{2m^{(\mathrm{M})}_{y_D}\left[(n+1)(1-\mathrm{P}^{(\mathrm{M})}_{H_s}\mathrm{P}^{(\mathrm{S})}_{H_s}) + (m-1)\mathrm{P}^{(\mathrm{M})}_{H_s}(1-\mathrm{P}^{(\mathrm{S})}_{H_s})\right]}{\mathrm{P}^{(\mathrm{M})}_{H_s}\mathrm{P}^{(\mathrm{S})}_{H_s}} \end{aligned} \tag{22}$$

Then, replacing (21) and (22) into (19) we get the final result.

The derivation of the service time at the slave unit is simplified by the fact that the slave never transmits DUPCKs, so that the transmission process renews itself at every MC step, irrespective of its state. A transmission attempt takes a time equal to $n+m$ if the slave is capable of correctly decoding the header of the master frame, and $n+1$ otherwise. The first–step analysis, then, returns

$$y^{(\mathrm{S})} = n+1+(m-1)\chi_{H_s^{(\mathrm{M})}} + (1-\chi_{H_s^{(\mathrm{M})}}\chi_{D_s^{(\mathrm{S})}})\tilde{y}^{(\mathrm{S})} \tag{23}$$

where, once again, $y^{(\mathrm{S})}$ and $\tilde{y}^{(\mathrm{S})}$ are identically distributed. Rising to the square and taking the expectations we, then, get

$$\begin{aligned} M_y^{(\mathrm{S})} = & \frac{(n+1)^2 + (m-1)\mathrm{P}^{(\mathrm{M})}_{H_s} + 2(n+1)(m-1)\mathrm{P}^{(\mathrm{M})}_{H_s}}{\mathrm{P}^{(\mathrm{M})}_{H_s}\mathrm{P}^{(\mathrm{S})}_{D_s}} \\ & + \frac{2m_y^{(\mathrm{S})}\left[(n+1)(1-\mathrm{P}^{(\mathrm{M})}_{H_s}\mathrm{P}^{(\mathrm{S})}_{D_s}) + (m-1)\mathrm{P}^{(\mathrm{M})}_{H_s}(1-\mathrm{P}^{(\mathrm{S})}_{D_s})\right]}{\mathrm{P}^{(\mathrm{M})}_{H_s}\mathrm{P}^{(\mathrm{S})}_{D_s}} \end{aligned} \tag{24}$$

Finally, the variance of the service delay, both at master and slave, can be obtained as

$$\sigma_y^2 = M_y - m_y^2$$

V. CASE STUDY

A. Model Accuracy

The correctness of the mathematical model has been checked by comparison with computer simulations. It shall be noticed that the mathematical model does not make any simplifying assumption in excess with respect to the simulation model. Therefore, the comparison was not intended to assess the accuracy of the analytical model with respect to a "real" case, but rather to double check the correctness of the equations. For this reason, this comparison has not been reported in the manuscript. Furthermore, we have compared our mathematical model with some previous literature, when possible. We observed that the goodput curves obtained through the model closely match with those reported in [8] for Bluetooth v1.0, except for a small discrepancy due to the inclusion in the model of the effect of the duplicate packets. Also, the statistics of the service delay derived in [16] for a half-symmetric piconet, with slaves sending $DH1$ packets and master sending only $POLL$ packets, correspond to what returned by (17) and (24) in the same scenario.

B. Reference scenarios

Since most of the data services that might be supported by Bluetooth networks generally produce asymmetric traffic flows, we will consider connections in which one unit transmits data frames whereas the other replies with control frames (either POLL or NULL) only. The symbols $(M \succ S)$ and $(S \succ M)$ are used to distinguish the case when data flow from master–to–slave and *vice versa*, respectively.

For fair comparison, the service delay is computed with respect to a reference PDU of size $L = \mathbb{D}(3, 5) = 1021$ byte, so that for a fixed frame format $\mathbb{D}(h, k)$, the mean and variance of the service delay are given by

$$m_\tau = \left\lceil \frac{L}{\mathbb{D}(h,k)} \right\rceil m_y \quad (25)$$

$${\sigma_\tau}^2 = \left\lceil \frac{L}{\mathbb{D}(h,k)} \right\rceil \sigma_y^2 \quad (26)$$

where $\lceil x \rceil$ is the ceiling function, which returns the smallest integer greater than or equal to x. For space limits, we will not report the results concerning the mean service delay, which is, in any case, proportional to the goodput metric. Instead, we will show the service delay variance, which is of interest for multimedia applications.

We model the energy consumption in transmission, reception and channel sensing, as the product of the overall power absorbed by the unit to perform the task and the time taken to complete it. This model has been proved valid for Bluetooth v1.1 by some experimental studies [34]. For convenience, we define a unit of energy (eu) as the amount of energy required for transmitting a bit at the basic rate. According to the results found in [34], we assume that the energy consumed in transmission, reception and channel sensing over a time interval $T_s = 1\mu s$ is equal to $P_{TX} \times T_s = 1\,eu$, $P_{RX} \times T_s = 0.8\,eu$ and $P_{SS} \times T_s = 0.1\,eu$, respectively, independently of the frame format used.

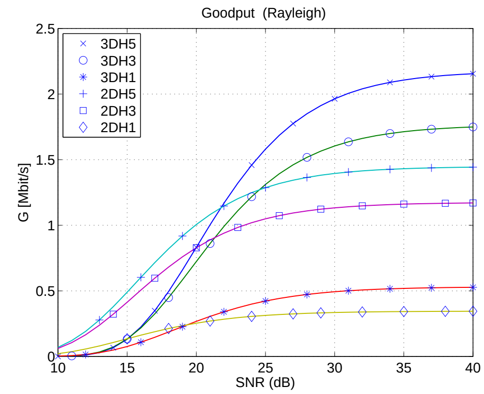

Figure 1. Goodput for $(M \succ S)$ data flows in Rayleigh channel.

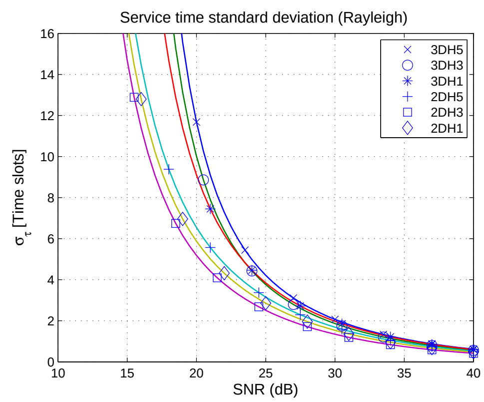

Figure 2. Standard deviation of the PDU service delay for $(M \succ S)$ data flows in Rayleigh channel.

For space constraints, we limit the analysis to Rayleigh channels, which represent an adverse scenario from the radio propagation perspective. Finally, we assume that the average Signal to Noise Ratio (SNR) is the same at both master and slave unit.

C. Performance analysis in fading channel

Fig. 1 and Fig. 2 show the average system goodput and the standard deviation of the PDU delay, respectively, versus SNR, for a $(M \succ S)$ connection. The energy efficiency and energy balancing curves in the same conditions are reported in Fig. 3 and Fig. 4, respectively. The six curves in each graph correspond to the different EDR frame formats used by the master, as indicated by the legend.

At a first glance, Fig. 1 shows that the best performance in terms of goodput is obtained by using $3DH5$ for SNR greater than 23 dB and $2DH5$ for lower SNR values. Shorter frame formats, however, might be used to transmit PDUs that do not fill the payload field of five–slot long frames.

Fig. 2 reveals that the standard deviation of the PDU service delay obtained with 3EDR frames is always greater than that obtained with 2EDR frames, despite a single PDU is fragmented into multiple 2EDR frames, as expressed in (26). The reason is that 3EDR formats are more likely to be retransmitted than 2EDR formats, thus increasing the randomness in

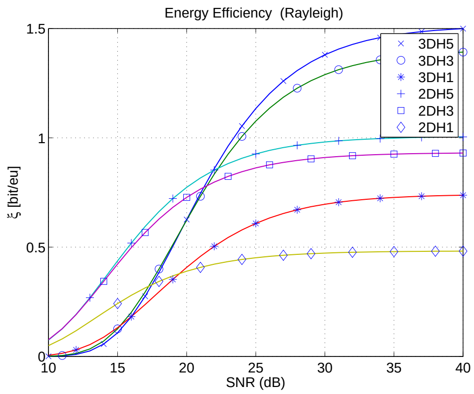

Figure 3. Energy efficiency for $(M \succ S)$ data flows in Rayleigh channel.

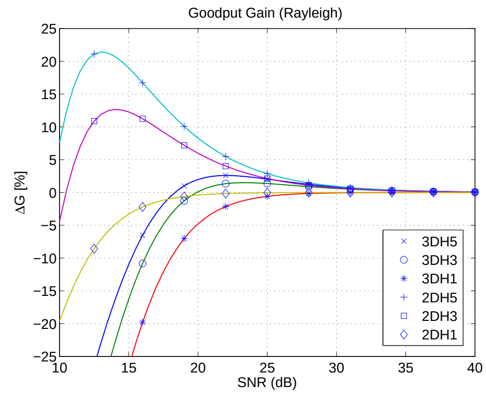

Figure 5. Goodput gain with $(S \succ M)$ configuration in Rayleigh channel.

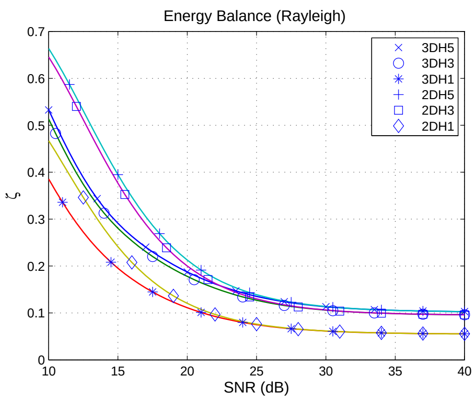

Figure 4. Energy balancing for $(M \succ S)$ data flows in Rayleigh channel.

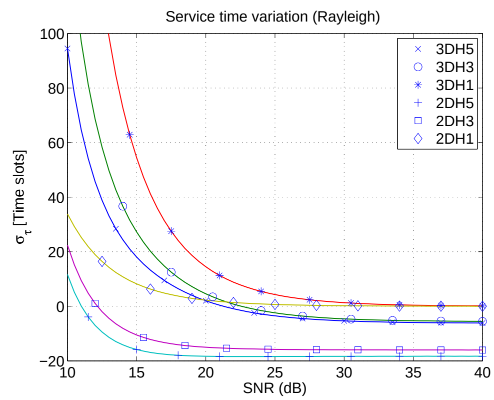

Figure 6. Delay standard deviation gain with $(S \succ M)$ configuration in Rayleigh channel.

PDUs service time. Nonetheless, the performance gap between frames of different size is rather narrow. This is due to the fact that, in fading channels, the frame size has a limited impact on the frame error rate, which is instead strongly affected by the random fluctuations of the channel gain.

The energy efficiency curves plotted in Fig. 3 show the same pattern observed for the gooudput, though the performance gap between 3DH5 and 3DH3, as well as between 2DH5 and 2DH3 frames, is limited. Therefore, from the energetic perspective, those frame formats are (almost) interchangeable. Concerning the energy consumption balancing, Fig. 4 shows a floor for high SNR values, which is due to the asymmetry of the connection and the different energy cost of transmitting and receiving. The sharp worsening of the energy balancing in the low SNR region is determined by the fact that, the lower the SNR, the higher the probability that the data frame contain unrecoverable errors in the AC or HEAD fields. In this case, the slave unit saves energy by stopping reception beforehand. The same argument also explains why the energy balancing for 2DH5 and 2DH3 is worse than for 3DH5 and 3DH3 formats in the low–SNR region, where 3EDR frames have very low energy efficiency, as shown by Fig. 3.

D. Swapping master and slave role

In the $(M \succ S)$ configuration it is possible for the master unit to transmit duplicate packets. These transmissions may represent an additional energy cost that might be avoided by assigning the slave role to the source node, i.e., adopting the $(S \succ M)$ configuration. To better appreciate the difference between $(S \succ M)$ and $(M \succ S)$ configurations, we introduce the *gain* metric for the goodput, delay standard deviation and energy efficiency, defined as follows:

$$\Delta\mathcal{G} = \frac{\mathcal{G}(S \succ M) - \mathcal{G}(M \succ S)}{\mathcal{G}(M \succ S)} \tag{27}$$

$$\Delta\xi = \frac{\xi(S \succ M) - \xi(M \succ S)}{\xi(M \succ S)} \tag{28}$$

$$\Delta\sigma_\tau = \frac{\sigma_\tau(S \succ M) - \sigma_\tau(M \succ S)}{\sigma_\tau(M \succ S)} \tag{29}$$

We do not define the gain for the energy balancing metric, which is by itself a relative index.

Fig. 5, Fig. 6 and Fig. 7 report the gain curves for the goodput, delay standard deviation and energy efficiency. For completeness, the energy balancing obtained for the $(S \succ M)$ configuration is reported in Fig. 8. We can notice that the $(S \succ M)$ configuration yields better performance than $(M \succ S)$ with some frame formats and worse with others. More in detail, single–slot formats always achieve lower goodput and energy efficiency, whereas $2EDR$ multislot frames experience up to 20% of goodput increment and 60% of energy efficiency

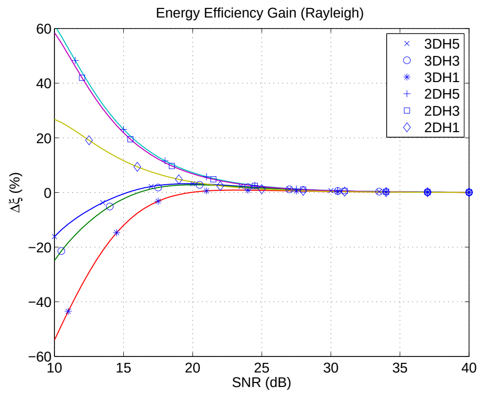

Figure 7. Energy efficiency gain for $(S \succ M)$ data flows in Rayleigh channel.

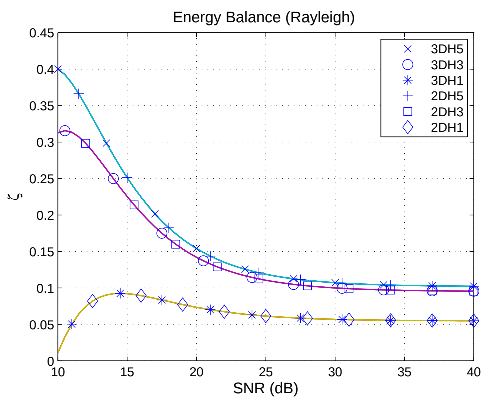

Figure 8. Energy balancing for $(S \succ M)$ data flows in Rayleigh channel.

gain. Multislot $3EDR$ formats, finally, show a limited performance gain for SNR greater than $20\,$dB, while they suffer severe performance loss for lower SNR values. In this SNR region, however, $3EDR$ frames are not suitable, since they achieve very low goodput also in the $(M \succ S)$ configuration, as shown in Fig. 1. Observing the results reported in Fig. 6, we see that the $(S \succ M)$ configuration yields lower delay variance in the high SNR region, in particular for $2DH5$ and $2DH3$ formats. Conversely, the delay variance increases in the low SNR region, in particular for $3EDR$ formats that, as already notice, are basically useless for these values of SNR. Finally, the $(S \succ M)$ configuration yields better (closer to zero) energy balancing, as it can be seen by comparing graphs of Fig. 8 and Fig. 4. However, it shall be noted that, with $(S \succ M)$ configuration, the most consuming unit is the slave, which is in charge for transmitting the data frames.

We observed similar results with other channel models, though the performance gain of $(S \succ M)$ configuration becomes progressively less significant as the channel model approaches AWGN.

VI. Conclusions

In this paper, we provided a mathematical model for the performance analysis of a Bluetooth data link, in terms of goodput, delay, energy efficiency and system lifetime. The model is based on an accurate analysis of the microscopic energy–saving mechanisms defined by Bluetooth standard, which have a significant impact on the overall performance figures of the system.

As a case study, we applied the model to an asymmetric data connection using EDR frame formats in Rayleigh fading channel. The study has revealed that, as expected, $3EDR$ frame formats yield better performance, both in terms of goodput and energy efficiency, in the high SNR ($> 23\,dB$) region, while $2EDR$ frame formats perform better in the low SNR region. However, $3EDR$ formats suffer higher delay variance over the entire SNR range (though the difference reduces as the Rice factor decreases).

Finally, in case of asymmetric data transfer, better performance is achieved by configuring the source node as slave and the destination unit as master. This configuration, in fact, yields better performance, provided that the suitable frame formats are used in each SNR region. However, the performance gain rapidly reduces for high SNR values and Rice factors, though for space contraints we have not reported the related performance curves.

We wish to remark that these considerations have been drawn for a specific case study. Therefore, applying the model to devices with different bit error rate figures and energy profiles, we might get discording results. In any case, the analytical framework here proposed remains valid, thus representing a useful tool for a detailed performance analysis of Bluetooth systems.

Appendix

Multi–slave scenario

Let us consider a piconet with n active slaves and, in turn, n asynchronous connectionless links. We assume the master adopts a simple round robin polling strategy according to which each slave is polled once per cycle, in a given order. Let $e_k \in \mathbf{E} = \{N, D\}$ denote the state of the k–th link, as defined in Sec. III, at the beginning of a polling cycle. The column vector $\mathbf{\Omega} = [e_k]_{k=1,\dots,n}$ is, then, the state of an n–dimensional Markov chain with state space $\mathbf{E}_n = \mathbf{E}^n$ and discrete steps corresponding to polling cycles. Following the footprints of Sec. III, we can determine the column vectors corresponding to the average time, data and energy rewards gained by each link over a polling cycle. Therefore, it is easy to realize that the time reward is the same for every link and it is obtained by summing up the n values returned by (7) for each link. Since transmission statistics on different links are mutually independent, the steady–state probability for the generic link k being in state N or D can still be obtained by plugging into (5) the frame formats and signal to noise ratios associated to link k. Hence, the master and slave data rewards for link k are still given by (8) and (9), respectively. The energy reward gained by the master over the generic link k can still be computed as given by (10). The energy reward of a slave unit, conversely, has to be augmented of the amount of energy spent by the unit during the polling of the other slaves. According to the standard, in fact, slaves are required to wake up at every reception slot to listen for a valid frame. However, slaves not addressed by the master are allowed to sleep till the end of the ongoing transmission, provided that AC and HEAD fields are correctly decoded. Hence, the average amount of energy $\Delta\overline{W}_k^{(S)}(h)$ spent by slave k during the service of link h, with $h \neq k$, is given by

$$\Delta\overline{W}_k^{(S)}(h) = w_{RX}(AC) + \mathrm{P}_{A_f}^{(M)}(k) w_{SS}(HEAD + PAYL^{(M)}) + \mathrm{P}_{H_f}^{(M)}(k) \left[w_{RX}(HEAD) + w_{SS}(PAYL^{(M)}) \right] + + \mathrm{P}_{H_s}^{(M)}(k) w_{RX}(HEAD) + \mathrm{P}_{H_s}^{(M)}(h) w_{RX}(AC) \left\lfloor \frac{m_h^{(S)}}{2} \right\rfloor \quad (30)$$

where $PAYL^{(M)}$ refers to the payload field of the frame format used by master over the h–th link, whereas $m_h^{(S)}$ is the slot length of the frame used by the h–th slave. All the terms in the right–hand side of (30), but the last, account for the energy spent by slave k to handle the master's frame intended for slave h. Conversely, the last term accounts for the energy spent by slave k checking the channel for a valid AC (every two slots) during the transmission of slave h. This term is weighted by the probability $\mathrm{P}_{H_s}^{(M)}(h)$ that slave h correctly decode the AC and HEAD of the master's frame, being then allowed to return its own frame. Finally, the overall energy reward for slave k is obtained by summing up the values returned by (30) for $h \neq k$, plus the energy consumed during the service of the link k, as given by (11).

REFERENCES

[1] *Specification of Bluetooth System, ver. 1.1*, February, 22 2001.

[2] *Specification Volume 2: Core System Package*, Bluetooth specification Version 2.0 + EDR ed., The Bluetooth Special Interest Group, 4 Nov. 2004.

[3] *Specification Volume 2: Core System Package*, Bluetooth specification Version 2.1 + EDR ed., The Bluetooth Special Interest Group, 26 July 2007.

[4] E. Fasolo, C. Prehofer, M. Rossi, Q. Wei, J. Widmer, A. Zanella, and M. Zorzi, "Energy-efficiency: challenges and new approaches for efficient data gathering and dissemination in pervasive wireless networks," in *Proc. of INTERSENSE06*, 2006.

[5] C. Ling-Jyh, S. Tony, and Y.-C. Chen, "Improving Bluetooth EDR data throughput using FEC and interleaving," in *The Second International Conference on Mobile Ad Hoc and Sensor Networks (MSN'06)*, 2006, pp. 725–736.

[6] G. Pasolini, M. Chiani, and R. Verdone, "Proposal of a MAC strategy for a Bluetooth based WLAN and performance evaluation in realistic channel conditions," *Proceedings of PIMRC'2001, S. Diego, CA*, Sep. 2001.

[7] ——, "Performance evaluation of a Bluetooth based WLAN adopting a polling MAC protocol under realistic channel conditions," *International Journal of Wireless Information Networks*, Apr. 2002.

[8] M. Valenti, M. Robert, and J. Reed, "On the throughput of Bluetooth data transmission," *Proc. IEEE WCNC, Orlando, FL*, Mar. 2002.

[9] D. Miorandi, A. Zanella, and G. Pierobon, "Performance evaluation of Bluetooth polling schemes: an analytical approach," *Mobile Networks and Applications*, vol. 9, no. 1, pp. 63–72, Feb. 2004.

[10] D. Miorandi, C. Caimi, and A. Zanella, "Performance characterization of a Bluetooth piconet with multi–slot packets," in *Proc. of WiOpt03*, Sophia–Antipolis, France, 2003.

[11] D. Miorandi and A. Zanella, "Achievable rate regions for Bluetooth piconets in fading channels," in *Proc. IEEE VTC (Spring)*, Milan, Italy, 2004.

[12] G. Zussman, A. Segall, and U. Yechiali, "On the analysis of the Bluetooth time division duplex mechanism," *Wireless Communications, IEEE Transactions on*, vol. 6, no. 6, pp. 2149–2161, June 2007.

[13] ——, "Bluetooth time division duplex - analysis as a polling system," *Sensor and Ad Hoc Communications and Networks, 2004. IEEE SECON 2004. 2004 First Annual IEEE Communications Society Conference on*, pp. 547–556, 4-7 Oct. 2004.

[14] J. Misic and V. Misic, "Modeling Bluetooth piconet performance," *Communications Letters, IEEE*, vol. 7, no. 1, pp. 18–20, Jan 2003.

[15] V. Misic and J. Misic, "On Bluetooth piconet traffic performance," *Personal, Indoor and Mobile Radio Communications, 2002. The 13th IEEE International Symposium on*, vol. 1, pp. 501–505 vol.1, 15-18 Sept. 2002.

[16] S. Y. Shin, H. S. Park, D.-S. Kim, and W. H. Kwon, "Performance analysis of single Bluetooth piconet in error–prone environments," *Journal of communications and networks*, vol. 9, no. 3, pp. 229–235, 2007.

[17] M. Kalia, D. Bansal, and R. Shorey, "MAC scheduling and SAR policies for Bluetooth: a master driven TDD pico-cellular wireless system," *Proc. of IEEE International Workshop on Mobile Multimedia Communications (MoMuC'99)*, Nov. 1999.

[18] ——, "MAC scheduling policies and SAR policies for Bluetooth MAC," *Proc. of IEEE VTC 2000–Spring, Tokyo*, 2000.

[19] K. Jang, T.-J. Lee, H. Kang, and J. Park, "Efficient power management policy in Bluetooth," *IEICE Transaction on Communications*, vol. E84-B, no. 8, pp. 2186–2192, August 2001.

[20] A. Zanella and M. Zorzi, "Throughput and energy efficiency of Bluetooth v2 + EDR in fading channels," in *IEEE Wireless Communications and Networking Conference (WCNC 2008)*, April 2008.

[21] J. Haartsen, "Bluetooth towards ubiquitous wireless connectivity," *Revue HF, Soc. Belge Ing. Telecommun. & Electron*, pp. 8–16, 2000.

[22] J. S. Roh, "Performance analysis and evaluation of Bluetooth networks in wireless channel environment," in *ICSNC '06: Proceedings of the International Conference on Systems and Networks Communication*. Washington, DC, USA: IEEE Computer Society, 2006, pp. 61–65.

[23] L. E. Miller and J. S. Lee, "BER Expressions for Differentially Detected $\pi/4$ DQPSK Modulation," *IEEE TRANSACTIONS ON COMMUNICATIONS*, vol. 46, no. 1, pp. 71–81, January 1998.

[24] N. Benvenuto and C. Giovanni, *Algorithms for Communications Systems and their Applications*. Wiley, 2002.

[25] A. Zanella, "A complete mathematical framework for the performance analysis of Bluetooth in fading channels," Dep. of Information Engineering, University of Padova, Italy, http://paduaresearch.cab.unipd.it/176/, Tech. Rep. 176, December 2007.

[26] A. Zanella, D. Miorandi, and S. Pupolin, "Mathematical analysis of Bluetooth energy efficiency," in *Proceedings of WPMC'03*, vol. 1, Yokosuka, Kanagawa, Japan, 19–20 Oct. 2003, pp. 152–156.

[27] A. Zanella, "Analysis of the packet reception statistics of Bluetooth v2+EDR in fading channels," Dep. of Information Engineering, University of Padova, Italy., http://paduaresearch.cab.unipd.it/155/, Tech. Rep. 112, September 2007.

[28] G. Stüber, *Principles of mobile communication*. Boston: Kluwer Academic, 1996.

[29] CSR, "Bluecore6-rom," www.csr.com.

[30] A. Chockalingam and M. Zorzi, "Energy efficiency of media access protocols for mobile data networks," *IEEE Transaction on Communications*, vol. 46, pp. 1418–1421, Nov. 1998.

[31] H. M. Taylor and S. Karlin, *An Introduction to stochastic modeling*. Academic Press, 1998.

[32] A. R. Howard, *Dynamic probabilistic systems*. Dover Publications, 2007, vol. I.

[33] M. Zorzi and R. R. Rao, "Energy constrained error control for wireless channels," *IEEE Personal Communications*, pp. 27–33, Dec. 1997.

[34] L. Negri, M. Sami, Q. D. Tran, and D. Zanetti, "Flexible power modeling for wireless systems: Power modeling and optimization of two Bluetooth implementations," in *WOWMOM '05: Proceedings of the Sixth IEEE International Symposium on a World of Wireless Mobile and Multimedia Networks (WoWMoM'05)*. Washington, DC, USA: IEEE Computer Society, 2005, pp. 408–416.